

INTERPRETING THE UNUSUALLY LONG TRANSIENT SIGNAL IN PHOTO-EXCITED METHYL VIOLOGEN IN WATER

A Senior Honors Thesis

Presented in Partial Fulfillment of the Requirements for graduation *with research distinction* in
Chemistry in the undergraduate colleges of The Ohio State University

by

Scott A. Suchyta

The Ohio State University
June 10, 2010

Project Advisor: Professor Bern Kohler, Department of Chemistry.

INTERPRETING THE UNUSUALLY LONG TRANSIENT SIGNAL IN PHOTO-EXCITED METHYL VIOLOGEN IN WATER

Scott A. Suchyta

The Ohio State University, Department of Chemistry, Columbus, OH 43210

June 10, 2010; Suchyta.2@buckeyemail.osu.edu

Abstract

The long-lived absorption observed in femtosecond transient absorption experiments at 295 nm when methyl viologen dication (MV^{2+}) is photo-excited in water at 266 nm has been assigned to a ground state MV^{2+}/OH^- ion pair. While a 1.68 μs lifetime component is seen in the 240 – 320 nm region, no accompanying change in IR absorption is observed. The assignment as a MV^{2+}/OH^- ion pair agrees with experiments showing that nitric acid quenches the long lived UV absorption.¹ Steady-state studies have produced the MV^{2+}/OH^- ion pair and difference spectra closely match the transient absorption results. A Ketelaar plot has determined the binding constant for MV^{2+} and a single hydroxide molecule to be $4.8 \pm 4.2 \times 10^{-2} M^{-1}$ and the change in molar extinction coefficient at 295 nm to be $5500 \pm 4900 M^{-1} cm^{-1}$, but further experiments should be performed to analyze and validate these values. It is proposed that the mechanism by which photo-excited MV^{2+} in water forms the MV^{2+}/OH^- ion pair can be described as concerted proton coupled electron transfer.

Introduction

Methyl viologen's (MV 's) role as an electron acceptor has been extensively studied. Fig. 1 shows the structure of MV^{2+} . It is a good redox indicator, and in a typical application an electronically excited donor species donates an electron to MV^{2+} in its ground state.² MV^{2+} is an even better electron acceptor in its first excited state.² Its excited state dynamics have been studied in several solvents, and it has been shown that the excited state lifetime is dependent on the solvent.² In methanol, which has an IP of 10.84 eV, the excited state lifetime of MV^{2+} is very short.² Forward electron transfer causes radical cation formation in less than 200 fs.² Eighty-eight percent of the MV returns to the ground state in 430 fs and long-lived radical cation is formed with a yield of 12%.² In acetonitrile (IP = 12.2 eV), no radical formation is observed and the decay of the excited state is slowed to 1 ns.² Changing the solvent to water, which has an even higher ionization potential (IP = 12.6 eV), produces different results.² The MV^{2+} excited state signal decays to zero in 3.1 ps, but if D_2O is used as the solvent, the lifetime increases to 5.3 ps.² There is no long-lived signal in the radical absorbing region around 600 nm. However, transient absorption (TA) with a lifetime of 1.68 μs is observed in the 240 - 320 nm region in fsTA experiments.^{1,2} This indicates that either a long-lived species other than the radical cation is formed or the ground state does not recover. Recently, it has been shown that the addition of acid to methyl viologen in water quenches the long-lived signal observed in TA studies at a rate of $3.1 \times 10^9 M^{-1}s^{-1}$.¹ This suggests formation of a MV^{2+}/OH^- ion pair as the long-lived species, but other possibilities exist. The purpose of the experiments presented here was to determine the identity of this long-lived transient signal in water.

As MV^{2+} has a relatively high electron affinity (EA = 1.2 eV)³, MV^{2+} acts as an acceptor molecule and forms charge transfer (CT) complexes with various Lewis-base type molecules.⁴ An anion is often the electron donor of the CT complex and several studies have focused on MV^{2+} /halide ion pairs.⁴⁻⁸ As described by Mulliken, the energy of a charge transfer transition is proportional to the IP of the donor and the EA of the acceptor.⁹ Experiments have shown that MV^{2+} charge transfer complexes are marked by increased absorption in the 290 – 400 nm region, and the exact energy of the new absorption depends on the identity of the donor molecule.^{4,7} Another spectral feature that has been observed upon MV^{2+} /halide ion pair formation is a decrease in absorption near 250 nm.⁵ For instance, Bertolotti, et al. has reported a negative band just below 250 nm in the MV^{2+}/Cl^- ion pair difference spectrum.⁵

When an ion pair, or more generally an association complex, is formed, the binding stoichiometry of the

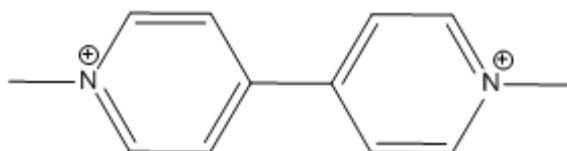


Fig. 1. Structure of methyl viologen dication (MV^{2+}).

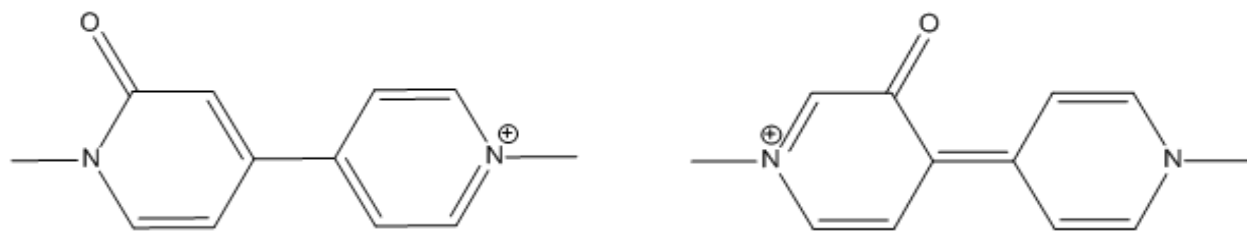


Fig. 2. Structures of pyridones derived from MV^{2+} . (a) 1',2'-dihydro-1',1'-dimethyl-2'-oxo-4,4'-bipyridylium (2-one) (b) 3,4-dihydro-1,1'-dimethyl-4,4'-bipyridylium (3-one)

complex can be determined through the use of a Job Plot.¹⁰ In this method, also known as the method of continuous variations, one varies the mole fractions of the two species forming the ion pair, while keeping total concentration constant.¹¹ A parameter proportional to complex formation (such as absorption) is measured and plotted against mole fraction of one of the species to determine the binding stoichiometry.¹¹ Given a 1:1 binding stoichiometry, several equations have been derived to determine the binding constant (K) and molar extinction coefficient (ϵ) of an association complex.¹²⁻¹⁵ In general, these methods assume the donor molecule of the charge transfer complex does not absorb in the region where the new charge transfer band appears. Simpler treatments, such as the Benesi-Hildebrand equation, also assume that the acceptor molecule of the complex does not absorb in the region of interest.¹² However, other methods of analysis, such as Rose-Drago or Ketelaar analysis, do not make this assumption.^{13, 14} An appropriate mode of analysis can be chosen based on experimental conditions and descriptions of the assumptions made in each approach can be found in literature.¹⁵ Using Benesi-Hildebrand analysis for instance, the K_1 value (the association constant corresponding to the binding of a 1:1 complex) for MV^{2+} with chloride, bromide, and iodide have been found to be 1.70, 3.40, and 3.80 M^{-1} , respectively.⁴

Oxidation of MV^{2+} to form pyridone products has also been described in the literature.¹⁶⁻¹⁸ Structures for the two pyridones derived from MV^{2+} are shown in Fig. 2, and the mechanisms by which they are formed are given in Fig. 3. Mau and coworkers attribute the green fluorescence seen after exciting solutions containing MV and other species at wavelengths greater than 310 nm at least in part to the pyridone 1',2'-dihydro-1',1'-dimethyl-2'-oxo-4,4'-bipyridylium (2-one).¹⁷ Under conditions where pH was greater than 9, the fluorescence increased with alkalinity and amount of time passed.¹⁷ The preparation of the 2-one has been described¹⁶ and its absorption and emission spectra are known.¹⁸ γ -irradiation of MV at pH 4 has also produced the 3-one, 3,4-dihydro-1,1'-dimethyl-4,4'-bipyridylium, and the absorption/emission of the 3-one has been reported.¹⁸ In these γ -radiolysis studies, the 2-one is the major product.¹⁸ The 3-one is produced to a larger extent when O_2 or Fe^{3+} is present, but the yield of both species drops upon the addition $FeCl_3$.¹⁸

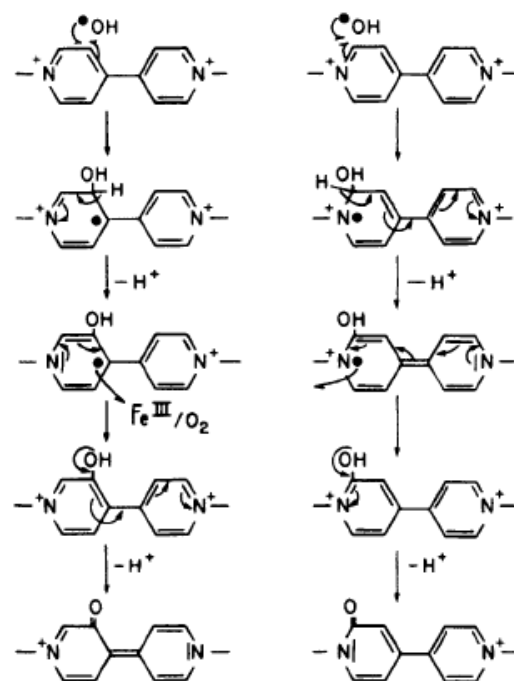


Fig. 3. Mechanisms by which the pyridones shown in Fig. 2 are formed.¹⁸

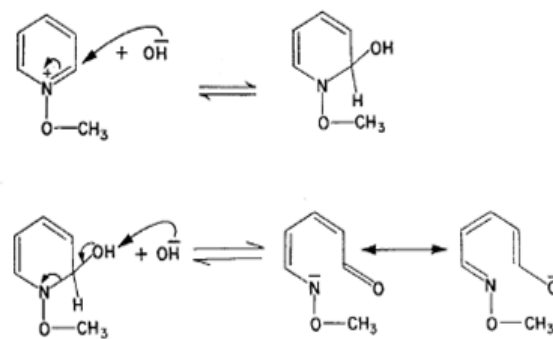


Fig. 4. Formation of a pseudo-base from N-methoxypyridinium.

As MV^{2+} is an unsaturated heterocyclic cation, it is prudent to consider the possibility of pseudobase formation when hydroxide is present. Under basic condition, many compounds similar to MV^{2+} , such as N-alkoxypyridinium cations, have been found to undergo pseudobase formation.¹⁹⁻²² Pseudobase production is characterized by hydroxide attaching to an aromatic ring by nucleophilic addition.²² Depending on the compound, the pseudobase may undergo ring opening to form the amino-carbonyl tautomer.²² Fig. 4 shows the mechanism of pseudobase formation starting with N-methoxypyridinium. In general, large changes to electronic spectra occur following pseudobase formation because the aromatic character of the ring is disrupted.²² However, even in very basic solutions, N-methylpyridinium cation (which is essentially half of MV^{2+}) has shown no spectral evidence of forming a pseudobase and there appears to be an ionic N-methylpyridinium hydroxide.²³

As stated above, the purpose of these experiments was to determine the identity of the long-lived transient species produced when MV^{2+} is photo-excited in water. The following logic was applied. Time-resolved infrared experiments were carried out to determine if a change in IR absorption accompanied the changes observed in transient absorption by UV-VIS. It was believed that this would provide evidence supporting or refuting the possibility of forming a pseudobase. As discussed in more detail later, if a pseudobase was the long-lived transient, one would expect to see a change in IR absorption upon its formation. Following the time-resolved studies, steady-state experiments were conducted in an attempt to reproduce the features observed in the TA spectrum of MV^{2+} in water. It was believed that if the long-lived product was the MV^{2+}/OH^- ion pair, it could be generated in steady-state experiments. Finally, if the long-lived species could be identified, it was hoped that these studies would provide insight into the mechanism by which the excited state of MV^{2+} relaxes when it is photo-excited in water.

Experimental

Samples. Methyl viologen dichloride hydrate (98%), D_2O (99.9 atom %), 1-butanol (99.9%), and KBr (99+%) were all purchased from Sigma-Aldrich and used as received. Sodium hydroxide (99%), sulfuric acid (95.6%), KI (100%), and Zn metal dust (100%) were purchased from Mallinckrodt and also used as received. $MV^{\bullet+}$ was prepared by chemically reducing solutions of MV^{2+} with Zn dust. All water was nanopure (≥ 18.0 M Ω -cm).

Time-Resolved Infrared (TRIR) Studies. nsIR studies were conducted using a previously described JASCO TRIR-1000 dispersive-type IR spectrometer with 16 cm^{-1} resolution.^{24, 25} Samples were held between two CaF_2 windows in a home-built flowcell and excited by 266 nm pulses. A solution of MV^{2+} in D_2O (3.80 mM) was prepared and analyzed in the 1500 – 1900 cm^{-1} and 1300 – 1420 cm^{-1} regions. For reference, MV^{2+} in butanol (4.06 mM) was also studied from 1500 – 1700 cm^{-1} . As the home-built flowcell required solvent to be added, some dilution of the samples occurred in each experiment, but this did not seriously impact the results. After dilution, the concentration of MV^{2+} in D_2O was approximately 1.75 mM.

The system used to perform the fsIR experiments has been described elsewhere.²⁶ Briefly, a sample of MV^{2+} in D_2O was held between two BaF_2 windows in a home-built spin cell with a 0.2 mm Teflon spacer. The solution was excited at 266 nm and probed in the 1600 – 1700 cm^{-1} region.

Steady-state Spectroscopy. Steady-state UV-VIS absorption spectra were taken on a Perkin Elmer Lambda 25 in a 1 mm quartz cell. For difference spectra, a stock solution of MV^{2+} was prepared and divided it into several aliquots. One aliquot was left unchanged and served as the reference solution. To the other aliquots, an appropriate amount of solid NaOH was added to achieve the desired OH^- concentration while keeping the MV^{2+} concentration identical to that of the reference solution. Difference spectra were generated by subtracting the reference solution spectrum from that of the solutions with NaOH added.

For neutralization experiments, stock solutions of 1.0 M and 10.860 M H_2SO_4 were prepared from concentrated sulfuric acid. Aliquots of these stock solutions were added to solutions containing known amounts of MV^{2+} and NaOH. Similarly, known amounts KBr were added to solutions containing known amounts of MV^{2+} and NaOH.

FTIR spectra were taken using a Perkin-Elmer Spectrum 2000 FTIR spectrometer. Samples were held between two CaF_2 windows in a spin cell with a 0.1 or 0.2 mm Teflon spacer. Solutions containing MV^{2+} and NaOH were made in an identical fashion to those used for the UV-VIS studies.

Emission measurements were made with a Spex Fluorolog 2 using excitation wavelengths of 267 and 385 nm. A solution containing about 4.8 mM MV^{2+} and 3 M NaOH was prepared and left exposed to light for three days. After the three days had passed, the solution was diluted by a factor of three and the absorption and emission of the spectrum were measured in a 1 cm path length cell.

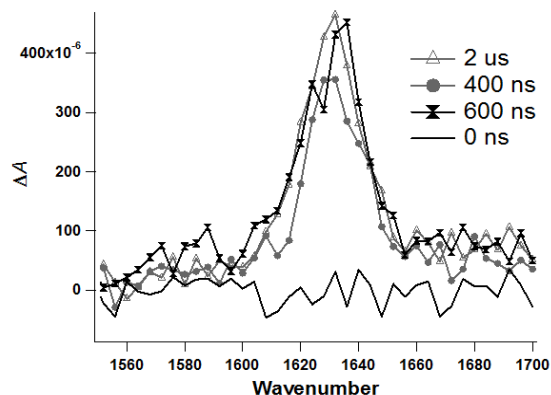


Fig. 5. Difference spectra following excitation of 4.06 mM MV^{2+} in D_2O at 266 nm at the indicated time delays.

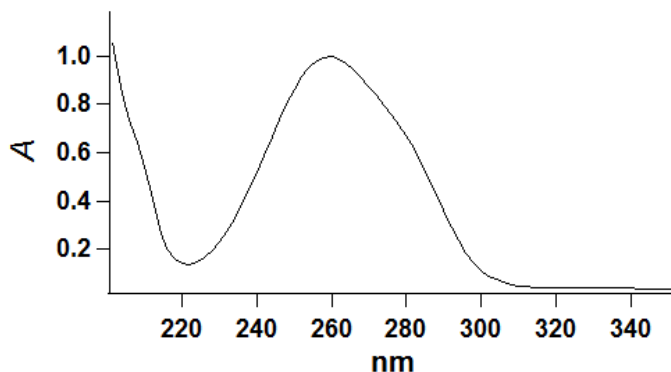


Fig. 6. Ground state absorption spectrum of 4.8 mM MV^{2+} in H_2O .

Fitting. Assigning the peak seen at 295 nm in the steady-state difference spectrum to MV^{2+}/OH^- ion pair formation (this assumption is justified in the Discussion section); the data at 295 nm were graphed according to the Ketelaar equation.¹⁴ The MV^{2+} concentration for these experiments ranged from 4.6 - 7.3 mM and the NaOH concentration ranged from 0.49 - 2.31 M. The form of the Ketelaar equation used was:

$$(1) \quad \frac{C_{MV}}{(A-A_0)/b} = \frac{1}{K \cdot \Delta\epsilon} \cdot \frac{1}{C_{OH}} + \frac{1}{\Delta\epsilon}$$

where A = absorption of the solution containing MV^{2+} and NaOH, A_0 = absorption of the solution containing just MV^{2+} , $\Delta\epsilon$ = molar extinction coefficient of MV^{2+}/OH^- CT absorption at 295 nm ($M^{-1}cm^{-1}$), K = the association constant for forming a 1:1 MV^{2+}/OH^- ion pair (M^{-1}), C_{OH} = concentration of hydroxide (M), C_{MV} = concentration of MV^{2+} (M), and b = path length of the cell (0.1 cm). The value of $C_{MV}/(A/b - A_0/b)$ for each trial were plotted as the y-values with $1/C_{OH}$ as the corresponding x-values and fit to a line using least squares fitting. According to this equation, the y-intercept is $1/\Delta\epsilon$ and the slope is $1/(K \cdot \Delta\epsilon)$.

Computational Studies. All calculations were performed using Gaussian '03 on the Glenn Cluster at the Ohio Supercomputer Center.²⁷ Gas phase MV^{2+} was first optimized with PM3. Using B3LYP/6-31+G*, the optimized PM3 structure was re-optimized and the vibrational frequencies were calculated. An MV pseudobase was built by adding a hydroxyl group to one of the ring carbon atoms that neighbors nitrogen in B3LYP optimized MV^{2+} structure. This pseudobase structure was then optimized and the vibrational frequencies were calculated with B3LYP/6-31+G*.

Results

TRIR Studies. Upon photo-excitation of MV^{2+} in butanol, an increase in absorption is observed around 1635 cm^{-1} in nsIR spectroscopy. IR difference spectra following 266 nm excitation are shown in Fig. 5. As photo-excited MV^{2+} is known to form $MV^{\bullet+}$ in butanol, the growth of the peak near 1635 cm^{-1} corresponds to radical formation and is consistent with previous studies.²⁸⁻³⁰ However, no transient signals are observed in ns or fsIR spectroscopy when MV^{2+} is photo-excited in D_2O .

Steady-state Spectroscopy. The ground state absorption spectrum of MV^{2+} has a maximum at 257 nm ($\epsilon = 20700\text{ M}^{-1}cm^{-1}$) in water.³¹ Fig. 6 is the spectrum of 4.8 mM MV^{2+} and compares well to previously published results.^{31, 32} A solution of MV^{2+} in water is clear, but upon addition of high concentrations of NaOH, it develops a yellow (slightly green) color. The intensity of this color increases as more NaOH is added and as more time has passed since the NaOH addition. Furthermore, after addition of NaOH, a small red-shift of the absorption peak at 257 nm occurs and there is a small increase in absorption at wavelengths greater 280 nm. It is easiest to observe these changes after the ground state absorption of MV^{2+} is subtracted from the absorption of the solution containing NaOH and MV^{2+} . The difference spectrum generated after adding 2.02 M NaOH to 0.73 mM MV^{2+} is shown in Fig. 7 in the 240 - 320 nm region. The difference spectrum is marked by a negative band around 255 nm and a positive band at 295 nm. Another small positive feature appears around 385 nm in the

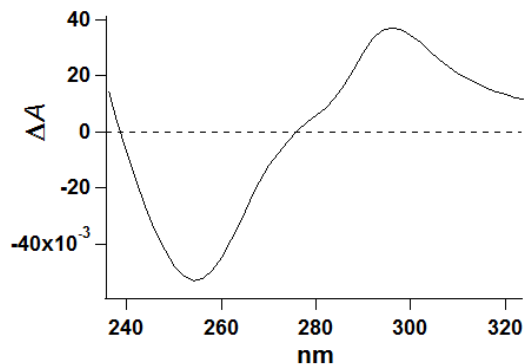


Fig. 7. Difference spectrum subtracting absorption of 0.73 mM MV^{2+} in H_2O from absorption of 0.73 mM $MV^{2+}/2.02$ M NaOH in H_2O .

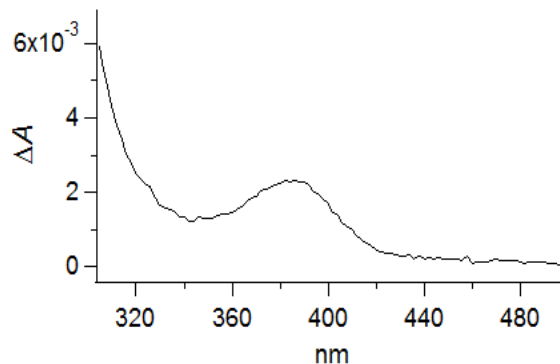


Fig. 8. Difference spectrum subtracting absorption of 0.46 mM MV^{2+} in H_2O from absorption of 0.46 mM $MV^{2+}/0.98$ M NaOH in H_2O .

difference spectrum. Fig. 8 shows the difference spectrum obtained when 0.98 M NaOH is added to 0.46 mM MV^{2+} in 320 – 500 nm region. Assignments for these bands are given in the Discussion section.

The ground state IR absorption of MV^{2+} has been characterized and is marked by strong absorption near 1649 cm^{-1} .^{33, 34} Fig. 9 is the FTIR spectrum of 8.2 mM MV^{2+} in D_2O and matches previously published results very well. $MV^{\bullet+}$ also absorbs in this region, with maximum absorption around 1640 cm^{-1} .²⁹ Fig. 10 shows the IR absorption of the radical cation in D_2O compared to MV^{2+} in D_2O . A significant increase in absorption occurs at 1640 cm^{-1} upon radical formation. The identification of the upper curve in Fig. 10 as the radical cation was confirmed by the UV-VIS absorption of the solution. The electronic spectrum is shown in Fig. 11 and matches previously published spectra of the radical.^{31, 35}

Upon addition of a large concentration of NaOH to MV^{2+} , there is an approximately 25 cm^{-1} shift to the strong ground state absorption band near 1650 cm^{-1} . Fig. 12 shows the IR absorption of a 2.9 mM MV^{2+} solution before and after addition of 0.53 M NaOH. The shifted band is centered at 1622 cm^{-1} and there appears to be little or no residual absorption where the MV^{2+} solution absorbed before hydroxide addition.

Fig. 13 shows the effects of adding different amounts of approximately 1 M H_2SO_4 to solutions containing about 4.7 mM MV^{2+} and 1 M NaOH. (The acid solution had the same concentration of H^+ as the $MV^{2+}/NaOH$ solution had of hydroxide.) As is necessary when a solution is diluted, the band centered at 385 nm decreased when increasing amounts of acid were added. When 1 mL of 10 M H_2SO_4 was added to 2 mL of a solution containing MV^{2+} and about 0.5 M NaOH (so that there was approximately ten times more H^+ than OH^- in the mixed solution), the band at 385 nm disappeared.

The electronic spectrum obtained after adding KBr to a solution containing MV^{2+} and NaOH is shown in Fig. 14. Upon addition of KBr, the amplitude of the peak at 257 nm decreases, but absorption in the 290 – 350 nm region increases. No changes are observed in the 370 – 450 nm region. These results are most clearly illustrated by the difference spectrum shown in Fig. 15.

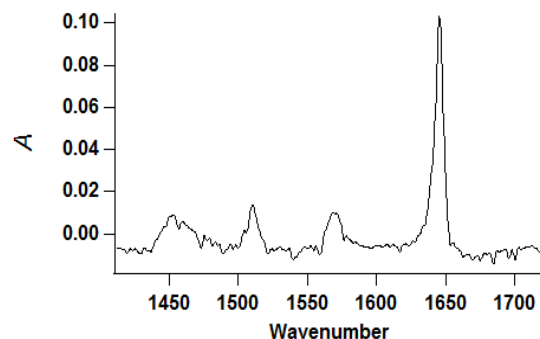


Fig. 9. Ground state FTIR spectrum of 8.2 mM MV^{2+} in D_2O .

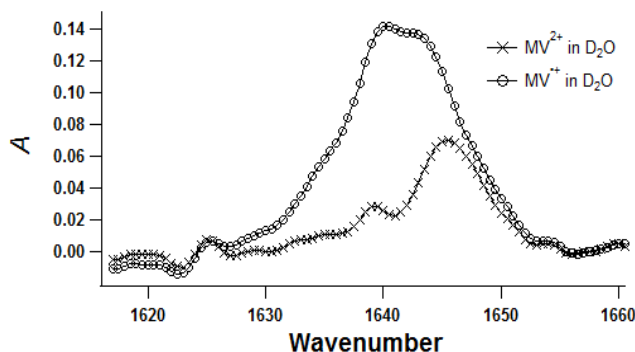


Fig. 10. FTIR spectra of 3.9 mM MV^{2+} in D_2O and $MV^{\bullet+}$ generated by adding Zn dust to 3.9 mM MV^{2+} in D_2O .

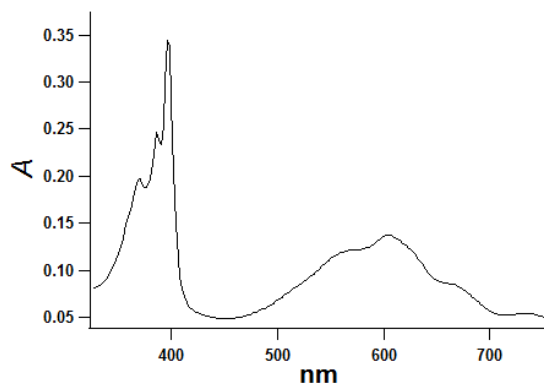


Fig. 11. UV-VIS absorption of $MV^{\bullet+}$ generated by adding Zn dust to 3.9 mM MV^{2+} in D_2O .

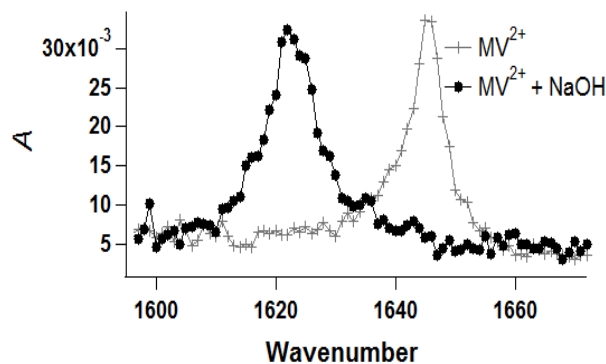


Fig. 12. FTIR spectrum of a 2.9 mM MV^{2+} solution before and after addition of 0.53 M NaOH.

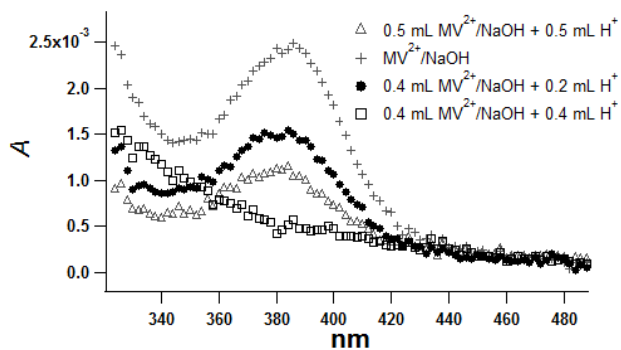


Fig. 13. UV-VIS spectra when the specified volume of 1 M H^+ was added to the specified volume of 4.7 mM MV^{2+} /1 M NaOH.

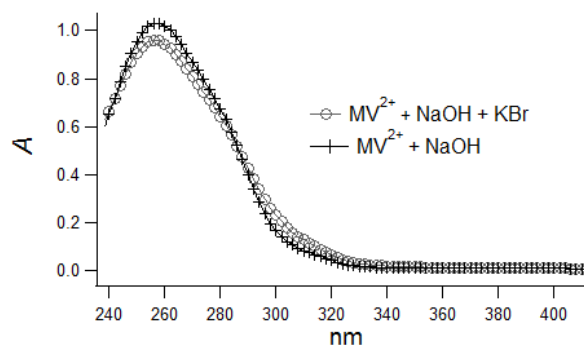


Fig. 14. UV-VIS spectra before and after addition of 1.02 M KBr to a 0.47 mM MV^{2+} /1 M NaOH solution.

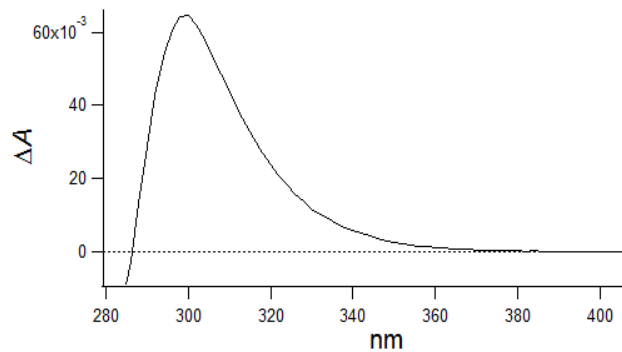


Fig. 15. Difference spectrum generated by subtracting absorption of a 0.47 mM MV^{2+} /1 M NaOH solution from absorption of a 0.47 mM MV^{2+} /1 M NaOH/1.02 M KBr solution.

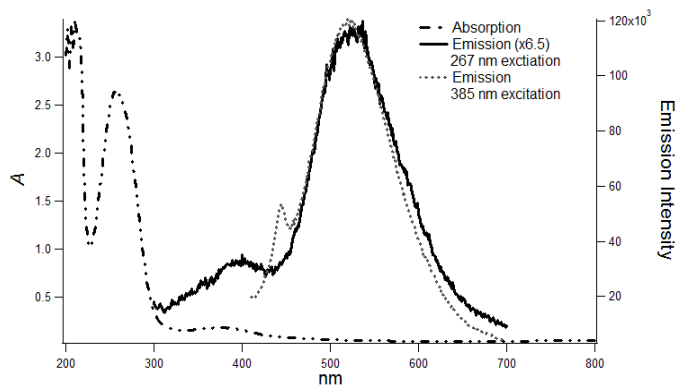


Fig. 16. Absorption and emission spectra of a MV^{2+} /NaOH solution that had been left exposed to light for three days. Emission spectra were excited at 267 and 385 nm.

The emission and absorption spectra of the diluted $MV^{2+}/NaOH$ solution that had been left exposed to light for three days are shown in Fig. 16. When exciting at 267 nm, the emission shows an intense peak near 525 nm. Another much less intense peak is centered at about 400 nm and tails off beyond 300 nm. Upon excitation at 385 nm, there is still an intense peak at 525 nm, but a second peak at 400 nm is not visible. The intensity of the peak at 525 nm was approximately 6.5 times more intense when exciting at 385 nm than at 267 nm.

Ketelaar Fit. Fig. 17 is a Ketelaar plot of the steady-state absorption data. The y-intercept is $1.8 \pm 1.6 \times 10^{-4} M^{-1}$ and the slope is $3.78 \pm 0.15 \times 10^{-3} M^2 cm$. Plugging in these values to solve for $\Delta\epsilon$ and then K in (1) yields values of $5500 \pm 4900 M^{-1} cm^{-1}$ for $\Delta\epsilon$ and $4.8 \pm 4.2 \times 10^{-2} M^{-1}$ for K . The meaning and validity of these values are explored in the Discussion section

Computational Studies. Using the parameters of di Matteo, the geometry of the optimized MV^{2+} structure is described in Table 1.³⁶ Since the results show good agreement with previous DFT calculations of MV^{2+} and with experiment, B3LYP seems well-suited for MV systems.^{36, 37} The five most intense vibrations calculated for MV^{2+} are given in Table 2 and compared to experimental values.³³ Once again, reasonably good agreement with experiment is observed and the vibrations fall within 50 wavenumbers or so of the true values. Table 3 shows the most intense vibrations calculated for the MV pseudobase (optimized structure shown in Fig. 18). Since the optimized geometrical parameters of the MV pseudobase were not essential to this study (calculating the vibrational frequencies was the chief priority), a full geometrical description is not given here but is available upon request.

The vibrational signature of the MV pseudobase is quite different than that of MV^{2+} . In general, the pseudobase has more intense vibrations than MV^{2+} in the 1500 – 1700 cm^{-1} range. Displacement vectors for the most intense MV^{2+} vibrations are shown in Fig. 19 (a), and displacement vectors for the most intense MV pseudobase vibrations are given in Fig 19 (b). These vibrations look very similar and correspond to approximately the same motion in the two molecules. However in changing from MV^{2+} to MV pseudobase, a slight shift to higher energies is seen and there is a large increase in intensity. Similarly, the vibration calculated at 1597 cm^{-1} for the pseudobase corresponds to the vibration calculated at 1595 cm^{-1} for MV^{2+} but has an intensity over six times as large. Therefore, the MV pseudobase has a vibrational spectrum that is distinct from MV^{2+} in the 1500 – 1700 cm^{-1} region.

Parameter ³⁶		Experimental ³⁷
$N_1 - C_2$	1.353 Å	1.344 Å
$C_2 - C_3$	1.387 Å	1.381 Å
$C_3 - C_4$	1.405 Å	1.391 Å
$C_4 - C_4'$	1.490 Å	1.481 Å
$C_1 - N_1$	1.492 Å	
$C_6 - N_2 - C_2$	120.3°	119.9°
$N_1 - C_2 - C_3$	121.0°	120.8°
$C_2 - C_3 - C_4$	120.0°	120.5°
$C_3 - C_4 - C_4'$	121.1°	121.3°
$C_3 - C_4 - C_5$	117.7°	116.6°
$C_2 - N_1 - C_1$	120.1°	
$C_2 - N_1 - C_6 - C_1$	0°	
ϕ	41.8°	

Table 1. Geometrical parameters of MV^{2+} optimized at B3LYP/6-31+G* level of theory.

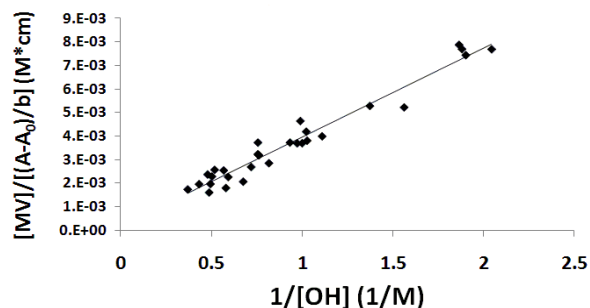
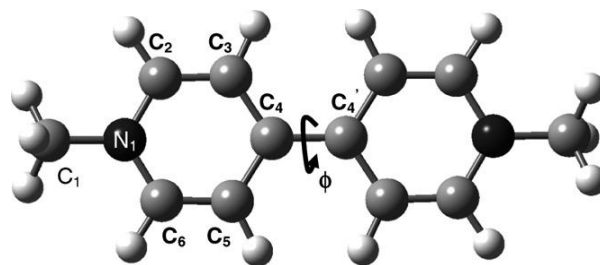


Fig. 17. Ketelaar plot for a series of solutions where the MV^{2+} concentration ranged from 4.6 - 7.3 mM and the NaOH concentration ranged from 0.49 - 2.31 M. (The y-intercept of the best fit line is $1.8 \pm 1.6 \times 10^{-4} M^{-1}$ and the slope is $3.78 \pm 0.15 \times 10^{-3} M^2 cm$.)



Calculated Frequency (cm^{-1})	Experimental Frequency (cm^{-1}) ³³	Calculated Intensity
1684	1643	193
1595	1563	49
1474	1445	36
1198	1143	47
849	825	83

Table 2. Most intense vibrations of MV^{2+} calculated with B3LYP/6-31+G*

Calculated Frequency (cm ⁻¹)	Calculated Intensity
1688	304
1597	292
1588	127
1218	146
945	80.

Table 3. Most intense vibrations of MV pseudobase calculated with B3LYP/6-31+G*

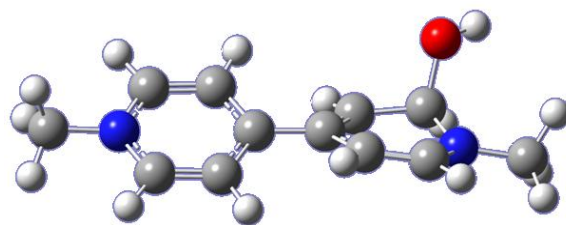


Fig. 18. Structure of MV pseudobase optimized with B3LYP/6-31+G*.

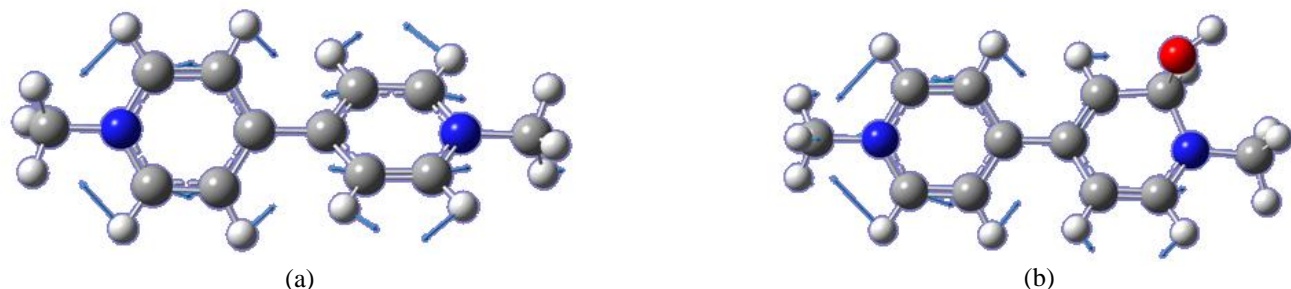


Fig. 19. Displacement vectors for the most intense vibrations calculated by B3LYP/6-31+G* for: (a) MV²⁺, (b) MV pseudobase

Discussion

TA spectra for MV²⁺ in water 1 ns after excitation at 266 nm match the steady-state UV-VIS absorption difference spectra in the 240 - 320 nm region very well.¹ Fig. 20 plots scaled results of these experiments. The remarkable agreement between the two suggests that the same species is producing the features observed in both spectra. This change in absorption in the 240 – 320 nm region has been assigned to a ground state MV²⁺/OH⁻ ion pair.

As support of ion pair formation, the difference spectrum in the 240 – 320 nm region looks very similar to difference spectra when MV²⁺ forms ion pairs with other anions, notably the MV²⁺/Cl⁻ difference spectrum reported by Bertolotti.⁵ In both cases, a negative band is observed near 250 nm and a positive band appears around 300 nm. Thus, the difference spectrum appears to have the qualitative features one would expect for a MV²⁺/OH⁻ ion pair.

The observation that the maximum absorption of the species occurs at 295 nm in TA and steady-state experiments is also consistent with MV²⁺/OH⁻ ion pair formation. The energy of CT peaks for MV²⁺ ion pairs can be predicted based on the IP of the donor molecule. Fig. 21 is a graph of IP in water for several anions that form ion pairs with MV²⁺ vs. the energy of maximum CT absorption in eV.^{5, 38} The maximum CT absorption for the OH⁻ data point was taken from the steady-state difference spectra data. From Fig. 21, it is clear that there is a linear relationship between IP of the anion and energy of the CT transition. This makes sense in terms of the Mulliken charge transfer model, which can be described by the equation

$$(2) \quad h\nu_{CT} = I_D - E_A + \Delta$$

where h is Planck's constant, ν_{CT} is the frequency of the transition, I_D is the IP of the donor, E_A is the electron affinity of the acceptor, and Δ is a correction term that accounts for differences in potential energy. Δ can be approximated as $\text{constant}/I_D - \text{constant}'$ for a series of donors with a single acceptor molecule.^{9, 39} Substituting this value for Δ yields a parabolic equation, but the curvature is generally rather small for the range of ionization potentials encountered for donors, so (2) can be approximated with the linear equation

$$(3) \quad h\nu_{CT} = a \cdot I_D - b$$

where a and b are empirical fitting parameters.^{4, 9} Thus it is logical that a plot of the energy of maximum CT absorption vs. IP of the donor for MV^{2+}/X^- ($X = I, Br, Cl, SCN$) would be a straight line. This line predicts that the MV^{2+}/OH^- ion pair should have maximum absorption at 294.6 nm, which agrees with the experimental data. Change in molar absorptivity at maximum CT absorption seems to follow a similar trend. Fig. 22 plots $\Delta\epsilon$ at maximum CT absorption for several MV^{2+} /anion ion pairs vs. IP of the donor.³⁸ Again, there appears to be a linear relationship, with the experimental MV^{2+}/OH^- data fitting on the line very well.

The TRIR results confirm that no long-lived $MV^{\bullet+}$ is formed in water. As shown by the studies of MV^{2+} in butanol, an increase in absorption should be seen around 1640 cm^{-1} in nsIR spectroscopy if long-lived cation radical is formed. The ground state vibration giving rise to the MV^{2+} absorption at 1649 cm^{-1} is the one depicted in Fig. 19 (a) (which was calculated to be at 1684 cm^{-1} by the B3LYP calculations) and corresponds to a ring vibration in which the two halves of the molecule are out of phase with one another.³⁰ When an electron is added to MV^{2+} to form the radical, the electron is delocalized over the molecule and shared between the two rings.³⁰ During the course of the vibration, electron density is partially localized on one half of the molecule.³⁰ The localization changes during the vibration, which results in a large change in dipole moment and produces a stronger vibrational mode.³⁰ Computations have predicted an approximately fourfold increase in intensity.³⁰ While a significant increase did occur, as is shown in Fig. 10, a fourfold increase was not observed upon radical cation formation in the steady-state IR experiments. One explanation for this is that care was not taken to exclude oxygen from the spin cell used to hold the sample. The radical cation can be oxidized by air, so complete radical generation likely did not occur.⁴⁰

Furthermore, the TRIR results provide strong evidence against the possibility of forming a pseudobase as the long-lived component. Based on the computational results, if this was to occur, one should see spectral changes in IR absorption. Specifically, significant increases in absorption should be observed in the 1500 – 1700 cm^{-1} region. Physically, spectral changes should be expected because the MV^{2+} ground state absorption at 1649 cm^{-1} is a ring vibration and attachment of hydroxide to one of the pyridine rings to form a pseudobase changes the ring structure.^{30, 33, 41} Since one of the rings would no longer be intact, large changes should also be observed if ring opening followed pseudobase formation. However, no long-lived changes in IR absorption are observed after MV^{2+} is photo-excited at 266 nm in D_2O and the complete decay of the signal at 1649 cm^{-1} in the fsIR and nsIR experiments requires the assignment that the long lived transient observed in time resolved electronic spectroscopy is due to a state has no vibrational signature corresponding to ring motions.

The assignment of the long-lived TA signal in water in the 240 – 320 region as the MV^{2+}/OH^- ion pair is consistent with the acid quenching results of Henrich. et al.¹ It has been found that the lifetime of the long-lived

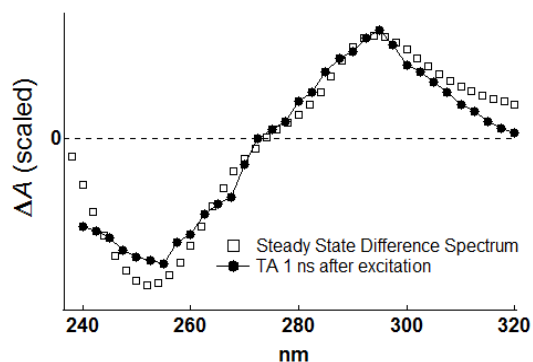


Fig. 20. Scaled comparison of difference spectrum in Fig. 7 to TA of MV^{2+} in H_2O 1 ns after excitation at 266 nm.

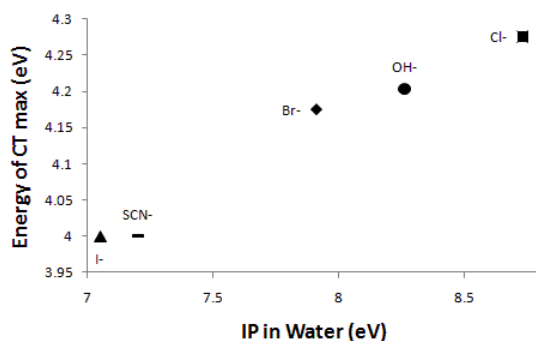


Fig. 21. Linear relationship between energy of maximum CT absorption³⁷ and IP of the anion for several MV^{2+} /anion ion pairs.⁵

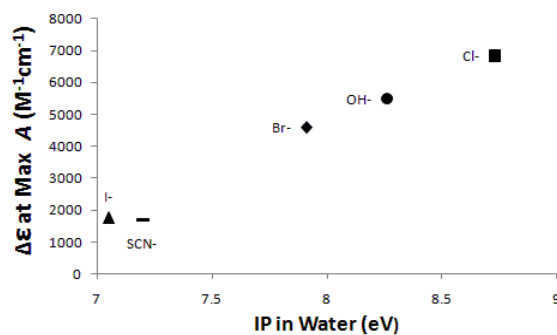


Fig. 22. Linear relationship between $\Delta\epsilon$ at maximum CT absorption³⁷ and IP of the anion for several MV^{2+} /anion ion pairs.⁵

species is quenched at a rate of $3.1 \times 10^9 \text{ M}^{-1} \text{ s}^{-1}$ when nitric acid is added to MV^{2+} in H_2O .¹ The simple explanation that after acid addition more protons are near the $\text{MV}^{2+}/\text{OH}^-$ ion pair and a proton can react with hydroxide to break up the ion pair offers insight into why this occurs. Thus, the shorter lifetime observed under acidic conditions agrees with ion pair formation.

The small band at 385 nm in the difference spectrum is assigned to pyridone absorption. This small positive feature is likely produced from a mixture of two different pyridones: 1',2'-dihydro-1,1'-dimethyl-2'-oxo-4,4'-bipyridylum (2-one) and 3,4-dihydro-1,1'-dimethyl-4,4'-bipyridylum (3-one). The 2-one is yellow and has an absorption maximum at 347 nm.¹⁸ The 3-one is green and is characterized by an absorption maximum at 392 nm.¹⁸ As the maximum in the steady-state difference spectrum is intermediate of the maxima for the 2-one and 3-one, forming a mixture of the two pyridones is consistent with the results. The gradual increase in absorption from 500 – 320 nm looks similar to the spectrum observed by Bahnemann in this region and suggests that other products are also being made in the steady-state experiments.¹⁸ No attempts were made to identify or quantify these other species. The emission spectrum of the $\text{MV}^{2+}/\text{NaOH}$ solution is also supportive of pyridone formation. MV^{2+} shows no emission when excited at 385 nm, so the intense peak at 525 nm must be due to something else. Accordingly, the emission at 525 nm agrees very well with pyridone emission described by Bahnemann.¹⁸ Similarly, the large difference in emission intensity at 525 nm when exciting at 385 and 267 nm indicates different species are primarily absorbing at 385 and 267 nm and further suggests pyridone has been formed. The emission in the 350 – 400 nm region when exciting at 267 nm matches previously observed MV^{2+} emission.² MV^{2+} emission is much weaker than pyridone emission, which accounts for the difference in sizes of the bands at 400 nm and 525 nm.

As pyridone production is occurring in the steady-state experiments, it is natural to question whether the increase in absorption at 295 nm in the difference spectrum could be due to pyridone formation. A simple examination of molar extinction coefficients eliminates this possibility. Fig. 23 shows the molar extinction coefficients of MV^{2+} , the 2-one, and the 3-one.¹⁸ At 295 nm, the molar extinction coefficient of MV^{2+} is larger than the molar extinction coefficient of either pyridone. Hence, pyridone production alone could not generate the positive feature seen the difference spectrum at 295 nm. In fact, pyridone formation would lead to a net decrease in absorption at 295 nm. This further supports the assignment of the band at 295 nm to the $\text{MV}^{2+}/\text{OH}^-$ ion pair. Theoretically, pyridone formation could contribute to the negative band around 250 nm in the difference spectrum. Indeed, the 3-one has a smaller ϵ value than MV^{2+} around 250 nm. However, as is evident from the very small magnitude of the band at 385 nm, a very small amount of pyridone is formed. Therefore, even though no attempts were made to quantify the amount of pyridone generated or the ratio of 2-one to 3-one, it is unlikely pyridone production could make a significant contribution to the negative band around 250 nm. By comparing molar extinction coefficients, the magnitude of the change in absorption due to pyridone formation near 250 nm could be no more than about four times greater than the change around 385 nm (which would occur if only the 3-one was produced). Even in this scenario, the actual magnitude of the observed change in absorption in the difference spectrum at 250 nm is well more than four times greater than the change at 385 nm. Thus the change due ion pair formation appears to be more significant. Assuming a mixture of pyridones is produced, which as previously mentioned seems most probable; the change in absorption at 250 nm corresponding to pyridone formation would be even less significant. Therefore, the features in the steady-state difference spectra from 240 – 320 nm can be predominantly attributed to ion pair formation with pyridone production contributing only a small amount to the negative band at 250 nm.

One can similarly question whether the absorption observed at 385 nm is truly from pyridone formation, or perhaps it is due to the $\text{MV}^{2+}/\text{OH}^-$ ion pair and happens to absorb in a similar region as the pyridones. This seems very improbable. In transient absorption studies, long-lived absorption is observed at 295 nm due to formation of the $\text{MV}^{2+}/\text{OH}^-$ ion pair but no long-lived signal is seen around 385 nm. If the band at 385 nm in the difference spectrum was due to ion pair formation, a positive peak should appear in the transient absorption spectrum at 385 nm. However, no such feature is observed. The results of adding KBr to a solution of MV^{2+} and NaOH seem to support the assignment of the absorption at 385 nm as pyridone as well. As is clear from Fig. 15, no change is seen to the band at 385 nm upon addition of KBr. Since Br^- is known to form an ion pair with MV^{2+}

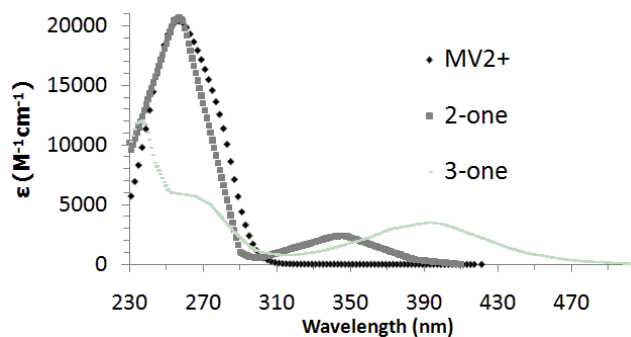


Fig. 23. Molar extinction coefficients for MV^{2+} , 1',2'-dihydro-1,1'-dimethyl-2'-oxo-4,4'-bipyridylum (2-one), and 3,4-dihydro-1,1'-dimethyl-4,4'-bipyridylum (3-one).¹⁸

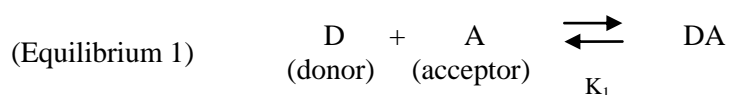
for which the association constant is much larger than the one determined for MV^{2+}/OH^- ($K_1 = 3.3 \text{ M}^{-1}$ for MV^{2+}/Br^-), bromide should preferentially form a CT complex with MV^{2+} compared to hydroxide. It seems this is occurring and is visible in the difference spectrum in Fig. 15 in the 280 – 340 nm region. The spectrum changes significantly after adding bromide and shows maximum change in absorption around 300 nm. As MV^{2+}/Br^- ion pairs have been found to have a maximum change in absorption at 297 nm, the experimental results seem to agree with preferentially forming the MV^{2+}/Br^- ion pair after bromide is added. Since the absorption at 385 nm does not change upon addition of the bromide and MV^{2+}/Br^- does not absorb at 385 nm, it does not seem logical that the band at 385 could be due to an MV^{2+}/OH^- ion pair.

The steady-state acid neutralization experiments were inconclusive. For the experiments where 1 M H^+ was added to solutions with MV^{2+} and 1 M OH^- it is difficult to tell if the decrease in the amplitude of the band at 385 nm is simply the result of dilution. For the addition of 0.5 mL H^+ to 0.5 mL MV^{2+}/OH^- and 0.2 mL of H^+ to 0.4 mL MV^{2+}/OH^- the change seems to be slightly more than what would be expected for simple dilution, but the magnitude of the change is so small that it is almost impossible to make any conclusions confidently. Perhaps as an argument against pyridone formation, when excess 1 M acid was added to MV^{2+} with 1 M NaOH, the band at 385 appears to have essentially disappeared. Similarly, the fact that the band at 385 nm completely disappeared in experiments where $>10 \text{ M } H^+$ was added to 1 M NaOH (the band would only have been expected to decrease by 33% from dilution) does not seem to support the assignment at 385 nm as pyridone. On the other hand, another possibility is that H^+ can react with pyridone. From the fluorescence studies, it seems very probable that the 385 nm peak is from pyridones. A reaction between H^+ and pyridone would seem to reconcile the results of the acid neutralization and emission experiments. However, proof of such a reaction was not the objective of these experiments and was not sought. To better quantify the results of the acid neutralization experiments, more tests would need to be done. Overall, the evidence for pyridone formation is still much stronger and the absorption at 385 nm has been assigned to pyridones. Although it would have been desirable, the acid neutralization experiments could not provide insight into confirming the increase in absorption at 295 nm as due to MV^{2+}/OH^- ion pair formation either. Since sulfate forms an association complex with MV^{2+} , the change in absorption at 295 nm could not be monitored as function of simple dilution.⁴

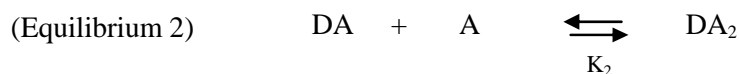
The cause of the shift in the FTIR spectrum upon addition of large quantities of NaOH to MV^{2+} has not been well identified but is believed to be due to some sort of a pH effect. From experimental data, it does not seem very likely that such an IR shift should occur upon formation of a MV^{2+}/OH^- ion pair. Solutions containing MV^{2+} and large excesses of either Cl^- or Br^- showed no shift in IR absorption compared to solutions without excesses of the anions. Also, no long-lived absorption was seen in TRIR studies in which the MV^{2+}/OH^- ion pair is believed to be formed. Thus, there does not seem to be convincing spectral evidence for IR shifts following MV^{2+} ion pair formation. Furthermore, the observed steady-state shift does not seem to be well explained by pyridone formation because there is no residual absorption at 1650 cm^{-1} . As discussed above, it seems only a small amount of pyridone is being formed. Therefore, even if a shift corresponding to pyridone production occurred, one would expect to see a large residual absorption at 1650 cm^{-1} from the MV^{2+} that has not formed pyridone. The most logical conclusion seems to be a pH effect but an accurate description for why this shift would occur is still unknown.

With the peak in the difference spectrum at 295 nm assigned to the MV^{2+}/OH^- ion pair, it is natural to attempt to determine details about the binding of MV^{2+}/OH^- . Ideally, the first step is to construct a Job Plot to determine the stoichiometry of the complex. This method is well described in literature.¹¹ One measures a parameter proportional to complex formation, absorption for instance, while varying the individual mole fractions of the two species forming the complex but keeping total concentration constant.¹¹ The parameter proportional to complex formation is then plotted against mole fraction of one of the components and the location of the maximum of this curve determines the binding stoichiometry of the complex.¹¹ However, this method requires that the total concentration of the species be much larger than the dissociation constant of the complex.¹¹ Otherwise, a Job Plot will always determine 1:1 stoichiometry.^{11, 42} As is indicated by the Ketelaar Plot of the steady-state data, the MV^{2+}/OH^- ion pair seems to have an association constant around 0.05 M^{-1} , which puts the dissociation constant on the order of 20 M. Using concentrations of MV^{2+} and OH^- of this magnitude was not feasible, so the method of continuous variations could not be applied.

Assuming 1:1 binding stoichiometry, one can utilize the Benesi-Hildebrand (BH) equation or one of its analogues, such as the Ketelaar equation or the Rose-Draco (RD) equation. These equations are derived from the general equilibrium expression:



One varies the concentrations of the donor and acceptor species and monitors absorption at the wavelength where the complex has maximum CT absorption to determine the K and ϵ values of the complex.^{13, 15} However, none of equations mentioned above taken into account the formation of 1:2 complexes described by



or the formation of any other higher stoichiometry complexes.

The BH equation was the first of these binding equations to be derived and many similar expressions utilizing different assumptions have followed. The BH equation is quite simple and expressed by

$$(4) \quad \frac{C_A \cdot b}{A} = \frac{1}{K \cdot \epsilon_c} \cdot \frac{1}{C_D} + \frac{1}{\epsilon_c}$$

where C_A is the concentration of the acceptor, C_D is the concentration of the donor, A is the absorption of the complex at the wavelength of interest, K is the binding constant for the 1:1 complex, ϵ_c is the molar extinction coefficient of the complex, and b is the path length of the cell.¹² This equation assumes that neither the donor nor the acceptor species absorbs in the region of complex absorption. In other words, only the complex absorbs in the region of interest.¹² The RD equation is the most general of these binding equations. It assumes the donor does not absorb at the maximum of complex absorption but allows for overlap of the acceptor and complex bands.¹³ The RD equation is given by

$$(5) \quad K^{-1} = \frac{\frac{A}{b} - \frac{A_0}{b}}{\epsilon_c - \epsilon_A} - C_A - C_D + \frac{C_D \cdot C_A}{\frac{A}{b} - \frac{A_0}{b}} (\epsilon_c - \epsilon_A)$$

where all of the variables are the same as previously defined and A_0 is the absorption of just the acceptor species at the wavelength of interest ϵ_A is the molar extinction coefficient of the acceptor.¹³

The Ketelaar equation (as well as the BH equation) is easily thought of as a simplification of the RD equation under certain conditions.¹³ The Ketelaar equation, which also allows for overlap of acceptor and complex absorption is

$$(6) \quad \frac{C_A}{A - A_0} = \frac{1}{K \cdot (\epsilon_c - \epsilon_A)} \cdot \frac{1}{C_D} + \frac{1}{(\epsilon_c - \epsilon_A)}$$

which is a simplification of the RD equation when the term $(A/b - A_0/b) / (\epsilon_c - \epsilon_A) - C_A$ is negligible compared to $(C_D \cdot C_A) \cdot (\epsilon_c - \epsilon_A) / (A/b - A_0/b) - C_D$.^{13, 14}

For the present experiments, the Ketelaar equation was chosen for analysis because experimental conditions were such that $(A/b - A_0/b) / (\epsilon_c - \epsilon_A) - C_A$ was negligible compared to $(C_D \cdot C_A) \cdot (\epsilon_c - \epsilon_A) / (A/b - A_0/b) - C_D$ when hydroxide was the donor molecule, MV^{2+} was the acceptor, and MV^{2+}/OH^- was the charge transfer complex. It is important to realize that 1:1 binding stoichiometry was assumed in this analysis. While MV^{2+} predominantly forms 1:1 complexes with anions at relatively low anion concentrations, K_2 values (as defined in Equilibrium 2) have been reported for MV^{2+}/Cl^- and I^- .^{4, 6} Thus, it is possible that MV^{2+} could form complexes with stoichiometries other than 1:1 with OH^- . To further evaluate this possibility, one could fit the absorption data assuming both Equilibrium 1 and Equilibrium 2. However, this was not done because there seemed to be a good linear fit assuming just Equilibrium 1. This suggests that formation of a 1:2 complex was not significant at the hydroxide concentrations used. Indeed, K_2 for MV^{2+} ion pairs is generally much smaller than K_1 and 1:2 complexes generally only become significant at higher anion concentrations,^{4, 6} so it seems reasonable that a 1:2 MV^{2+}/OH^- species would not form to an appreciable extent. A good future experiment would be to use a larger range of hydroxide concentrations and see if/at what concentrations a second equilibrium

expression is required to adequately fit the data. This could establish when higher binding is significant and confirm that only 1:1 complexes were formed to an appreciable extent over the concentrations used in these experiments. Overall from the experimental results, it seems very probable that only 1:1 MV^{2+}/OH^- ion pairs were produced, but more work is needed to establish this definitively.

The determined K_1 value of 0.048 M^{-1} for the MV^{2+}/OH^- ion pair is very small. K_1 values for other MV^{2+} /anion ion pairs are shown in Table 1.⁵ One hypothesis for the low value is that hydrogen bonding can lower the value of the equilibrium constant. The hydroxide of the MV^{2+}/OH^- ion pair can hydrogen bond strongly with the water solvent. As a result, complexation to form the ion pair must compete with hydrogen bonding, effectively reducing the binding

constant. Since anions such as chloride, bromide, and iodide do not participate in hydrogen bonding, it would seem reasonable that they have higher association constants. However this description does not seem to be complete when the K_1 values of CN^- and SCN^- , each of which can hydrogen bond with water, are considered. Each of these anions has an association constant that is at least an order of magnitude larger than that of OH^- , which is not consistent with the hydrogen bonding hypothesis. Therefore, it is probable that a more detailed explanation than simple hydrogen bonding is needed to fully describe the qualitative trends in K_1 .

It should be noted that the uncertainties in K ($4.8 \pm 4.2 \times 10^{-2}\text{ M}^{-1}$) and $\Delta\epsilon$ ($5500 \pm 4900\text{ M}^{-1}\text{ cm}^{-1}$) for the MV^{2+}/OH^- ion pair are very large compared to the magnitudes of measurements themselves. This occurred because the y-intercept of the Ketelaar fit was very close to zero. With such a small y-intercept, small changes to the best fit line cause proportionally large changes in the y-intercept, which significantly alter the calculated values of $\Delta\epsilon$ and K . Therefore, when the y-intercept of a Ketelaar plot is close to zero, $\Delta\epsilon$ and K are extremely sensitive to changes in the y-intercept, and it is difficult to determine small binding constants using Ketelaar analysis.

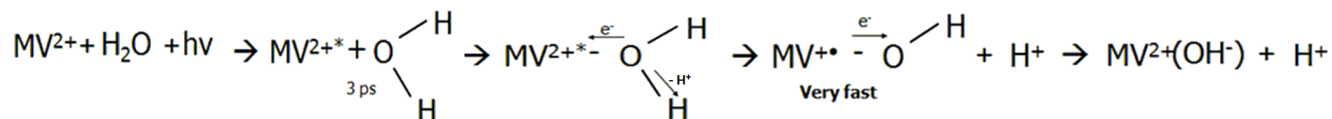
Given these problems with the Ketelaar fit, some effort was made to perform Rose-Drago analysis.¹³ However, these efforts were generally unsuccessful. It was difficult to reproduce results from one day to the next, and consistent values of K and $\Delta\epsilon$ were not obtained. These problems were not entirely surprising though and difficulties and inconsistencies in applying RD analysis (and more broadly BH type analysis in general) to determine the binding of weakly bound complexes have been encountered.^{43, 44} In some cases, BH type methods may only be capable of determining the product of K and $\Delta\epsilon$ and not be able to reliably determine their values independently.⁴³ As mentioned, for the steady-state UV-VIS absorption experiments, RD analysis did not yield consistent results from one experiment to another, so it is believed the method was not suitable for determining K and $\Delta\epsilon$ independently and further RD analysis was abandoned.

With these limitations and the fact that Ketelaar analysis is another BH type method in mind, the reported K and $\Delta\epsilon$ values for the MV^{2+}/OH^- ion pair should be questioned, and the validity of the Ketelaar equation for MV^{2+} /anion systems in general should be explored. Following the exact same procedures used to generate the steady-state difference spectra of MV^{2+}/OH^- , solutions containing MV^{2+} associated with Cl^- , Br^- , and I^- should be made and studied using Ketelaar analysis. If such experiments yield K and $\Delta\epsilon$ values similar to previously published results, the method would be validated in a general sense for the systems being studied. Furthermore, other more sophisticated methods for determining the binding of complexes with low association constants exist.^{43, 44} To more accurately determine the binding of the MV^{2+}/OH^- ion pair, these modes of analysis could be applied.

Finally, it is appropriate to comment on the mechanism by which the MV^{2+} excited state decays when MV^{2+} is photo-excited in water. The excited state lifetime is 3.1 ps in water and 5.3 ps in D_2O .² This isotope effect indicates that a proton coordinate must be involved in the decay mechanism. Furthermore, there is no spectral evidence of radical cation formation. The TRIR studies show no increase in absorption at 1650 cm^{-1} . Although TA studies in both water and methanol show positive peaks around 400 and 600 nm after photo-excitation, the shapes and ratios of the peaks are different, indicating that different species are being monitored.² In water, the long-lived signal in the 240 – 320 nm region has a lifetime of 1.68 μs , and has been assigned as the MV^{2+}/OH^- ion pair.¹ Given this information, the proposed stepwise mechanism is shown in Scheme 1 and includes concerted proton coupled electron transfer (PCET). After photo-excitation, a lone pair on the oxygen of water associates with MV^{2+*} . Simultaneous to electron transfer from water to MV^{2+*} , a proton dissociates from water to the bulk solvent. The gas phase IP of water (12.6 eV) is too high for MV^{2+*} to simply oxidize the water. However, the proton transfer event lowers the energy needed to take an electron from water, so electron transfer

Anion	$K_1\text{ (M}^{-1})^5$
Cl^-	1.7 ± 0.9
Br^-	3.3 ± 0.2
I^-	3.9 ± 0.2
CN^-	0.71 ± 0.04
SCN^-	2.0 ± 0.1

Table 1. K_1 values for the association of MV^{2+} with several anions.



Scheme 1. Proposed mechanism for photo-excitation of MV^{2+} in water.

becomes possible if the proton also dissociates. It is believed that the 3.1 and 5.3 ps lifetimes correspond to the time required for solvent rearrangement in H_2O and D_2O , respectively. After PCET, MV radical cation and a hydroxyl radical are formed but only exist for a very short amount of time. As mentioned, there is no spectral evidence for radical formation in water. Therefore, it is proposed that back electron transfer occurs from $\text{MV}^{+\bullet}$ to the hydroxide radical faster than the time resolution of the experiments to form the $\text{MV}^{2+}/\text{OH}^-$ ion pair. As indicated by acid quenching TA experiments H^+ recombines with the hydroxide of the ion pair at a rate of $3.1 \times 10^9 \text{ M}^{-1}\text{s}^{-1}$.¹ In neat water, H^+ and OH^- recombine at a rate of $1.4 \times 10^{11} \text{ M}^{-1}\text{s}^{-1}$.⁴⁵ This slower recombination can be explained by Coulombic factors. H^+ and OH^- recombination in neat water is rapid because it involves oppositely charged species. In the system containing MV^{2+} though, $(\text{MV}/\text{OH})^+$ must recombine with H^+ . Each of these is a positively charged species, so it makes sense they would recombine much more slowly. The PCET mechanism presented here is very interesting and is described in greater detail elsewhere.¹

Conclusions

MV^{2+} has been shown to form a ground state $\text{MV}^{2+}/\text{OH}^-$ ion pair when it is photo-excited in water at 266 nm via concerted proton coupled electron transfer. Accordingly, acid can react with the hydroxide of the ion pair and nitric acid quenches the long-lived signal at a rate of $3.1 \times 10^9 \text{ M}^{-1}\text{s}^{-1}$.¹ The energy of maximum absorption for the $\text{MV}^{2+}/\text{OH}^-$ ion pair coincides with predictions based on Mulliken CT theory. As shown by Fig. 20, steady-state difference spectra of the ion pair match the TA data very well. While more work is warranted, the association constant for the $\text{MV}^{2+}/\text{OH}^-$ ion pair has initially been found to be $4.8 \pm 4.2 \times 10^{-2} \text{ M}^{-1}$. This is a very weak association constant, and perhaps can be explained in part because OH^- can hydrogen bond strongly with the water solvent. The corresponding $\Delta\epsilon$ at 295 nm should also be interpreted cautiously and has been determined to be $5500 \pm 4900 \text{ M}^{-1} \text{ cm}^{-1}$. According to Fig. 22, $\Delta\epsilon$ agrees well with values for other MV^{2+} /anion ion pairs. The fact that no long-lived changes in IR absorption are observed after photo-excitation of MV^{2+} eliminates the possibilities of forming a pseudobase as the long-lived state. Therefore, it has been concluded that the 1.68 μs lifetime component characterized by transient absorption in the 240 – 320 nm region is due to the formation of the $\text{MV}^{2+}/\text{OH}^-$ ion pair.

Acknowledgments

This work was supported in part by allocation of computing time from the Ohio Supercomputer Center. I thank Drs. Bern Kohler and Terry Gustafson and graduate students Joe Henrich, Kimm de La Harpe, Charlene Su, Yu Kay Law, and Jinquan Chen for their support and suggestions. I would also like to thank thesis committee members Drs. Dutta, Hadad, and Cao.

References

1. Henrich, J. D., Suchyta, S. A., Kohler, B. K., Manuscript in Preparation.
2. Peon, J.; Tan, X.; Hoerner, J. D.; Xia, C. G.; Luk, Y. F.; Kohler, B., Excited state dynamics of methyl viologen. Ultrafast photoreduction in methanol and fluorescence in acetonitrile. *Journal Of Physical Chemistry A* **2001**, 105, (24), 5768-5777.
3. White, B. G., Bipyridylum Quaternary Salts And Related Compounds. 3. Weak Intermolecular Charge-Transfer Complexes Of Biological Interest, Occurring In Solution And Involving Paraquat. *Transactions Of The Faraday Society* **1969**, 65, (560P), 2000-&.
4. Monk, P. M. S.; Hodgkinson, N. M.; Partridge, R. D., The colours of charge-transfer complexes of methyl viologen: effects of donor, ionic strength and solvent. *Dyes And Pigments* **1999**, 43, (3), 241-251.

5. Bertolotti, S. G.; Cosa, J. J.; Gsponer, H. E.; Previtali, C. M., Charge-Transfer Complexes Of Diquat And Paraquat With Halide Anions. *Canadian Journal Of Chemistry-Revue Canadienne De Chimie* **1987**, 65, (10), 2425-2427.
6. Jarzeba, W.; Pommeret, S.; Mialocq, J. C., Ultrafast dynamics of the excited methylviologen-iodide charge transfer complexes. *Chemical Physics Letters* **2001**, 333, (6), 419-426.
7. Ebbesen, T. W.; Ferraudi, G., Photochemistry Of Methyl Viologen In Aqueous And Methanolic Solutions. *Journal Of Physical Chemistry* **1983**, 87, (19), 3717-3721.
8. Kunkely, H.; Vogler, A., Optical charge transfer in the ion pairs methyl viologen(2+) guanosine-5'-monophosphate(2-) and adenosine-5'-triphosphate(2-). *Chemical Physics Letters* **2001**, 345, (3-4), 309-311.
9. Mulliken, R., Molecular complexes: a lecture and reprint volume. **1967**.
10. Job, P., Job's method of continuous variation. *Annali di chimica applicata* **1928**, 10, (9).
11. Huang, C. Y., Determination Of Binding Stoichiometry By The Continuous Variation Method - The Job Plot. *Methods In Enzymology* **1982**, 87, 509-525.
12. Benesi, H. A.; Hildebrand, J. H., A Spectrophotometric Investigation of the Interaction of Iodine with Aromatic Hydrocarbons. *Journal of the American Chemical Society* **1949**, 71, (8), 2703.
13. Rose, N. J.; Drago, R. S., Molecular Addition Compounds of Iodine. I. An Absolute Method for the Spectroscopic Determination of Equilibrium Constants. *Journal of the American Chemical Society* **1959**, 81, (23), 6138.
14. Ketelaar, J. A. A., von de Stolpe, C., Goud-Smit, A., Dzugas, W., *Rec. trav. chim.* **1952**, 71, 1104.
15. Zubov, A. V., Ivanova, T.V., Approximate equations for the determination of complexing parameters: Applicability. *Journal of Solution Chemistry* **1982**, 11, (10), 699-717.
16. Calderba, A.; Charlton, D. F.; James, R.; Farrington, J., Bipyridylum Quaternary Salts And Related Compounds. 4. Pyridones Derived From Paraquat And Diquat. *Journal Of The Chemical Society-Perkin Transactions 1* **1972**, (1), 138-&.
17. Mau, A. W. H.; Overbeek, J. M.; Loder, J. W.; Sasse, W. H. F., On The Fluorescence And Photoreduction Of Methyl Viologens. *Journal Of The Chemical Society-Faraday Transactions II* **1986**, 82, 869-876.
18. Bahnmann, D. W.; Fischer, C. H.; Janata, E.; Henglein, A., The 2-Electron Oxidation Of Methyl Viologen - Detection And Analysis Of 2 Fluorescing Products. *Journal Of The Chemical Society-Faraday Transactions I* **1987**, 83, 2559-2571.
19. Eisenthal, R.; Katritzky, A., Ring-Opening Of N-Methoxypyridinium Perchlorate By Hydroxide Ion. *Tetrahedron* **1965**, 21, (9), 2205-&.
20. Katritzky, A.; Lunt, E., N-Oxides And Related Compounds. 35. Reactions Of N-Alkoxy-Pyridinium And -Quolinium Cations With Nucleophiles. *Tetrahedron* **1969**, 25, (18), 4291-&.
21. Schneck, J.; Heber, D., Reactions Of N-Alcoxycyclimonium Salts. 2. Heterocycles From Ring-Opening Reactions Of N-Methoxypyridinium Salts. *Tetrahedron* **1974**, 30, (22), 4055-4057.
22. Bunting, J. W., Heterocyclic Pseudobases. *Advances in Heterocyclic Chemistry* **1980**, 25, 1-82.
23. Serpone, N., Ponterini, G., and Jamieson, M. A., Covalent hydration and pseudobase formation in transition metal polypyridyl complexes: reality or myth? *Coordination Chemistry Reviews* **1982**, 50, 209-302.
24. Hare, P. M.; Middleton, C. T.; Mertel, K. I.; Herbert, J. M.; Kohler, B., Time-resolved infrared spectroscopy of the lowest triplet state of thymine and thymidine. *Chemical Physics* **2008**, 347, (1-3), 383-392.
25. Martin, C. B.; Tsao, M.-L.; Hadad, C. M.; Platz, M. S., The Reaction of Triplet Flavin with Indole. A Study of the Cascade of Reactive Intermediates Using Density Functional Theory and Time Resolved Infrared Spectroscopy. *Journal of the American Chemical Society* **2002**, 124, (24), 7226.
26. Middleton, C. T., Dissertation: Vibrational and excited-state dynamics of DNA bases revealed by UV and infrared femtosecond time-resolved spectroscopy. **2008**.
27. Gaussian 03, R. D., M. J. Frisch, G. W. Trucks, H. B. Schlegel, G. E. Scuseria, M. A. Robb, J. R. Cheeseman, J. A. Montgomery, Jr., T. Vreven, K. N. Kudin, J. C. Burant, J. M. Millam, S. S. Iyengar, J. Tomasi, V. Barone, B. Mennucci, M. Cossi, G. Scalmani, N. Rega, G. A. Petersson, H. Nakatsuji, M. Hada, M. Ehara, K. Toyota, R. Fukuda, J. Hasegawa, M. Ishida, T. Nakajima, Y. Honda, O. Kitao, H. Nakai, M. Klene, X. Li, J. E. Knox, H. P. Hratchian, J. B. Cross, V. Bakken, C. Adamo, J. Jaramillo, R.

- Gomperts, R. E. Stratmann, O. Yazyev, A. J. Austin, R. Cammi, C. Pomelli, J. W. Ochterski, P. Y. Ayala, K. Morokuma, G. A. Voth, P. Salvador, J. J. Dannenberg, V. G. Zakrzewski, S. Dapprich, A. D. Daniels, M. C. Strain, O. Farkas, D. K. Malick, A. D. Rabuck, K. Raghavachari, J. B. Foresman, J. V. Ortiz, Q. Cui, A. G. Baboul, S. Clifford, J. Cioslowski, B. B. Stefanov, G. Liu, A. Liashenko, P. Piskorz, I. Komaromi, R. L. Martin, D. J. Fox, T. Keith, M. A. Al-Laham, C. Y. Peng, A. Nanayakkara, M. Challacombe, P. M. W. Gill, B. Johnson, W. Chen, M. W. Wong, C. Gonzalez, and J. A. Pople, Gaussian, Inc., Wallingford CT, 2004.
28. Peon, J., Unpublished manuscript. **2001**.
 29. Brienne, S. H. R.; Cooney, R. P.; Bowmaker, G. A., Infrared Spectroelectrochemical Evidence For Alkyl Viologen Radical Monomers In Acetonitrile. *Journal Of The Chemical Society-Faraday Transactions* **1991**, 87, (9), 1355-1359.
 30. Brienne, S. H. R.; Boyd, P. D. W.; Schwerdtfeger, P.; Bowmaker, G. A.; Cooney, R. P., Intensity Enhancements In The Ir-Spectra Of Organic Radical Ions - A Theoretical-Study. *Journal Of The Chemical Society-Faraday Transactions* **1993**, 89, (16), 3015-3020.
 31. Watanabe, T.; Honda, K., Measurement Of The Extinction Coefficient Of The Methyl Viologen Cation Radical And The Efficiency Of Its Formation By Semiconductor Photocatalysis. *Journal Of Physical Chemistry* **1982**, 86, (14), 2617-2619.
 32. Yuen, S. H.; Bagness, J. E.; Myles, D., Spectrophotometric Determination Of Diquat And Paraquat In Aqueous Herbicide Formulations. *Analyst* **1967**, 92, (1095), 375-&.
 33. Poizat, O.; Sourisseau, C.; Mathey, Y., Vibrational Study Of The Methyl Viologen Dication Mv^{2+} And Radical Cation Mv^+ In Several Salts And As An Intercalate In Some Layered Mps3 Compounds. *Journal Of The Chemical Society-Faraday Transactions I* **1984**, 80, 3257-3274.
 34. Ito, M.; Sasaki, H.; Takahashi, M., Infrared spectra and dimer structure of reduced viologen compounds. *The Journal of Physical Chemistry* **1987**, 91, (15), 3932.
 35. Wolszczak, M.; Stradowski, C., Methylviologen Cation Radical, Its Dimer And Complex In Various Media. *Radiation Physics And Chemistry* **1989**, 33, (4), 355-359.
 36. di Matteo, A., Structural, electronic and magnetic properties of methylviologen in its reduced forms. *Chemical Physics Letters* **2007**, 439, (1-3), 190-198.
 37. Bockman, T. M.; Kochi, J. K., Isolation And Oxidation Reduction Of Methylviologen Cation Radicals - Novel Disproportionation In Charge-Transfer Salts By X-Ray Crystallography. *Journal Of Organic Chemistry* **1990**, 55, (13), 4127-4135.
 38. Takahashi, N.; Sakai, K.; Tanida, H.; Watanabe, I., Vertical Ionization-Potentials And Ctts Energies For Anions In Water And Acetonitrile. *Chemical Physics Letters* **1995**, 246, (1-2), 183-186.
 39. Bender, C. J., Theoretical-Models Of Charge-Transfer Complexes. *Chemical Society Reviews* **1986**, 15, (4), 475-502.
 40. Rieger, A. L.; Edwards, J. O., Methyl Viologen Reactions.5. Rates And Mechanism Of Cation-Radical Formation In Aqueous Base. *Journal Of Organic Chemistry* **1988**, 53, (7), 1481-1485.
 41. Hester, R. E.; Suzuki, S., Vibrational Analysis Of Methylviologen. *Journal Of Physical Chemistry* **1982**, 86, (23), 4626-4630.
 42. Huang, C. Y.; Zhou, R. X.; Yang, D. C. H.; Chock, P. B., Application of the continuous variation method to cooperative interactions: mechanism of Fe(II)-ferrozine chelation and conditions leading to anomalous binding ratios. *Biophysical Chemistry* **2003**, 100, (1-3), 143-149.
 43. Zaini, R.; Orcutt, A. C.; Arnold, B. R., Determination of equilibrium constants for weakly bound charge-transfer complexes. *Photochemistry And Photobiology* **1999**, 69, (4), 443-447.
 44. Yang, C.; Liu, L.; Mu, T. W.; Guo, Q. X., Improved accuracy and efficiency in the determination of association constants with the spectrophotometric method. *Journal Of Inclusion Phenomena And Macrocyclic Chemistry* **2001**, 39, (1-2), 97-101.
 45. Eigen, M., The influence of steric factors in fast protolytic reactions as studied with HF, HQS, and substituted phenols. *Journal of American Chemical Society* **1960**, 82, 5952-5953.